Article

An Enhancement of Compositional Stability of Phase Change Materials by Lamination with Aluminum Sheet

Nithusha Kallingal [1], Patrik Sobolčiak [1], Himyan Mohammed Akbar [1], Igor Krupa [1], Igor Novak [2] and Anton Popelka [1,*]

[1] Center for Advanced Materials, Qatar University, Doha P.O. Box 2713, Qatar
[2] Polymer Institute of the Slovak Academy of Sciences, 845 41 Bratislava, Slovakia
[*] Correspondence: anton.popelka@qu.edu.qa; Tel.: +974-4403-5676-l

Abstract: The wax leakage from shape-stabilized phase change materials (SSPCMs) is a limitation because it reduces their functionality. In this work, an enhancement of the compositional stability of SSPCMs formed by high-density polyethylene (HDPE) and paraffin wax blends through a lamination by aluminum (Al) foil was studied. The materials' thermal conductivity was enhanced by adding expanded graphite (EG). The lamination of SSPCMs is the simplest method of reducing leakage, but it suffers from poor adhesion between polymer-based blends and protecting layers. The improved adhesion between SSPCMs and Al foil was achieved by adding 2 wt.% of maleated polyethylene (PE) acting as an adhesion promoter into SSPCMs or by plasma treatment of both SSPCMs and Al surfaces. Microscopic, spectroscopic, and optical techniques were used to analyze the surface and adhesion properties of SSPCMs. The peel resistance of SSPCMs after plasma treatment or modification by maleated PE increased from 2.2 N/m to 7.2 N/m or 55.1 N/m, respectively. The wax leakage from the treated or modified SSPCMs was suppressed significantly. The plasma-treated or maleated PE-modified SSPCMs showed leakage of 0.5 wt.% or 0.2 wt.%, respectively, after three days of leakage test. It indicates a good potential of this treatment/modification for industrially applied SSPCMs.

Keywords: PCMs; plasma; maleated polyethylene; paraffin wax; adhesion; leakage

1. Introduction

It has been estimated that the building and construction industry consumes just for heating and cooling approximately 30%–40% of the world's total energy produced from fossil fuels resulting in one-third of the world's greenhouse gas emissions [1]. For this reason, it is important to develop materials that effectively absorb and release excess thermal energy to ensure indoor thermal comfort, with minimal electrical energy for heating in winter and cooling in summer. These materials reduce variations in the temperature of buildings during temperature changes over a day without needing external energy sources.

In general, these materials are called thermal energy storage (TES) materials, and they can be efficiently installed into interiors and exteriors of buildings and constructions to substitute the consumption of electrical energy. For this reason, they currently have attracted considerable attention in the construction industry. The current and future challenges regarding R&D and commercialization of TES products for large-scale applications were critically discussed in a recent review paper by Gunasekara et al. [2].

Phase change materials (PCMs) belong to the most prospective TES materials applicable in building or solar-aided applications [3–5]. PCMs are materials that can undergo phase transition between solid to liquid phase at a specifically selected temperature while absorbing or releasing a high amount of energy, which is proportional to their specific enthalpy of melting. For this reason, they can absorb/release energy in the form of sensible heat and as a latent heat associated with the phase transition of (semi)crystalline structures, significantly enhancing their efficiency. Different inorganic and organic substances, such

are inorganic salts (e.g., polyhydric alcohols), fatty acids, and paraffin waxes can be used as PCMs [6]. However, paraffin waxes are the most promising ones due to their favorable characteristics, such as a high enthalpy of melting/crystallization, a broad range of melting temperatures–dependent on the number of carbons in the paraffinic chain, stability, negligible super-cooling, availability, and a relatively low price [7]. Furthermore, wax has a high specific enthalpy of melting (latent heat) ranging from 180 to 230 kJ/kg, resulting in excellent energy storage density [8,9].

Wax undergoes a solid–liquid phase transition during melting, and thus, they tend to leak from the space where they were installed. The leakage represents one of the most crucial obstacles in installing PCMs products within construction. The simplest and oldest way to prevent this undesirable circumstance is to store the wax in closed tanks or containers; however, using air-tight containers has disadvantages [9–12].

Alternatively, wax can be fixed in a stable form by encapsulation within a polymeric shell, emulsion polymerization, or mixing with certain polymers [13–21]. For example, wax within a thin polymeric (or silica) shell completely suppresses leakage. However, it reduces the active component (wax) content in the system, especially if microcapsules are mixed with concrete, plaster, or polymers, which results in a significant decrease in energy sorption efficiency [22].

Direct mixing of certain polymers with wax is another approach that enables the incorporation of much higher wax content into a material. Different polymeric matrices can be used for this purpose; however, the most common ones are various grades of PE. This is because they can reduce post-melting leakage, the extent of which is dependent on the compatibility of wax and PE components. The resulting materials are referred to as shape-stabilized SSPCMs. PE is the most frequently used polymer for blending with wax because of their chemical and structural similarity [23,24], which allows a large amount of wax (up to 60 wt.%) to be incorporated into the PE matrix. However, even under these conditions, there is some wax leakage if materials undergo several melting/crystallization cycles because of the wax diffusion from the bulk to the outer surfaces. This phenomenon leads to a decrease in wax content within PCMs over time and therefore decreases PCM functionality. This happens because, despite the chemical and structural similarity of wax and PE, most PE grades are not fully miscible with wax, especially in the crystalline phase [25].

Some exceptions exist; for instance, linear low-density PE blended with certain high-molar Fisher–Tropsch waxes have shown miscibility in both amorphous and crystalline phases [26,27]. However, these blends cannot be implemented as shape-stabilized PCMs because they have one melting temperature only, and materials collapse (completely melts) once this temperature is obtained and materials (products) lose their important feature–shape stability unless they are chemically cross-linked [27].

Thus, an efficient method to prevent wax leakage must be developed for the large-scale application of these materials [28]. In this paper, we describe an efficient and straightforward treatment of SSPCMs surfaces through a lamination by Al foil, where the improved adhesion was ensured by (i.) an addition of maleated PE into high-density PE (HDPE) and (ii.) plasma treatment of both SSPCMs and aluminum foil surfaces. SSPCMs reported in this paper are designed from HDPE as a matrix, wax as a practical phase change component, and expanded graphite (EG) serving as a filler, which enhances the thermal conductivity of materials, and additionally partly reduces the wax leakage. In addition, EG also suppresses degradation behavior under light (UV) exposition. Various physical features of such materials were discussed in our previous papers [29,30].

The search on the current global market for PCMs purposed for construction works indicated just one producer and product, where lamination of products was performed by attachment of Al foil. This manufacturer is DuPont, who has developed the product DuPont™ Energain®. It is a panel consisting of a copolymer that serves as the matrix, and wax, which acts as the phase-change component and is dispersed throughout the matrix. The transition between the solid and melted phase (i.e., the target temperature) occurs at

approximately 18 °C, the wax content of the final material is 60 wt.%, and the latent heat capacity is 70 J/g. A thin Al layer further covers these sheets to prevent wax leakage [31].

This paper deals explicitly with the suppression of wax leakage from polymeric SSPCMs through the lamination of products with aluminum foil. Wax leakage is suppressed by combining suitable additives (maleated polyethylene) with HDPE and wax and plasma treatment of both SSPCMs samples and Al foil before making the joint between them. Plasma treatment and a small amount of added maleated polymer are realizable at a large, industrial scale and can be easily implemented in various applications, such as in the building industry. To our knowledge, no paper has been published in the literature investigating this topic. SSPCMs used for this purpose are formed from HDPE, wax, and EG, and their thermal properties are only briefly summarized here, as they are not relevant to this paper.

This work has a very special focus on dealing with the suppression of leakage of Wax from SSPCMs (from polymer/wax mixtures in general) through the lamination of products with Al foil. The problems are associated with the poor adhesion between PE/wax blends and Al foil. The presence of wax within a structure makes the problem more challenging in comparison with simple polymer/Al structures due to the continuous diffusion of wax to the interface. This interfacial adhesion improvement is ensured by a combination of suitable additives (maleated PE) compounded together with HDPE, wax and EG or by plasma of both SSPCMs samples and Al foil prior to making the joint between them. We did not find any paper in the scientific literature investigating this topic. As for the commercial product, the most known is Dupont's Energain system, but it differs from our system in many aspects. This panel is composed of 40 wt.% of ethylene-copolymer and 60 wt.% of wax, and no fillers enhancing thermal conductivity are added. The panel of 5 mm thickness panel is covered by Al foil. The melting point is 22 °C, and the heat storage capacity of the panels is 515 kJ/m^2 [32].

2. Materials and Methods

2.1. Materials

HDPE (Q-Chem, Qatar) with MFI 2.1, paraffin wax RT42 (Rubitherm$^®$ Technologies GmbH, Berlin, Germany) with melting, expanded graphite with an average particle size (D50) of 200 µm SGL (Carbon's SIGRATHERM$^®$, Berlin, Germany), maleated PE (OREVAC$^®$ 18302N, SK Functional Polymer, Paris, France) were used for the preparation of PCMs.

2.2. SSPCM Blends Preparation

The SSPCM blends were prepared by mixing the required proportion of HDPE, wax, and EG (50/50/0, 48/50/2, 45/50/5, 43/50/7, 40/50/10) based on our previous studies [33] in a 50 mL mixing chamber of a Brabender$^®$ Plastograph$^®$ EC W50 PLE 331 (Duisburg, Germany) for 15 min at 160 °C and at mixing speed of 35 rpm. The selected blend (40/50/10) was additionally modified by adding 2 wt.% of OREVAC, and mixtures were prepared at the same conditions. The samples of the required shape were prepared from homogeneously mixed blends using a hydraulic mounting press machine (Carver 3895, Wabash, IN, USA) by hot pressing for 5 min at 160 °C and with subsequent cooling down to room temperature (RT) by water medium. The densities of blends have been calculated by additive rule [34].

2.3. Lamination Preparation

Laminate consisted of the maleated PE-modified HDPE/Wax/EG, and the plasma-treated Al foil was fabricated to suppress wax leakage from the SSPCMs system. Primarily, HDPE/Wax/EG samples were placed into a square frame stainless steel mold (1 mm thick), and laminate structure was obtained by applying two plasma-treated Al foils on the top and bottom sides of HDPE/Wax/EG using a mounting hot press machine. Followed by heating, pressing (10 min at 160 °C), and cooling down the sample to RT. The resulting laminates were cut to desired shapes and used for further analyses.

2.4. Plasma Treatment

Plasma treatment of the HDPE/Wax/EG sample and Al foil was conducted using the low-temperature plasma generating system Venus75-HF (Plasma Etch Inc., Carson, CA, USA). A radio-frequency (RF) generator (frequency-13.56 MHz) generated homogeneous plasma in the reactor. A vacuum pump was used to reduce pressure in the chamber to ~26.6 Pa. The HDPE/Wax/EG and Al foil were placed in the cylindrical chamber of the plasma reactor, and both sides were exposed to RF plasma discharge for 60 s at a nominal power of 80 W generated in the air.

2.5. Thermal Properties Analyses

Differential scanning calorimetry (DSC) was carried out by a PerkinElmer DSC 8500 (Shelton, CT, USA) differential scanning calorimeter. First, the specimens were heated from 0 to 60 °C at a constant heating rate of 5 °C/min and then cooled down at the same heating rate and heated up again to eliminate the thermal history of the samples. The thermal properties were obtained from the second heating run. All measurements were repeated at least three times, and average values with standard deviations were obtained. The procedure was adopted based on a previous publication [35].

In the case of the specific heat capacity measurement, the sample was cooled to 15 °C at a rate of 5 °C/min, held at this temperature for 2 min, then heated to 65 °C and held at it for 2 min. Nitrogen gas was passed through the instrument at a flow rate of 20 mL/min. DSC software was used for calculating specific heat capacity (c_p) values as a three-step method, where baseline, sapphire, and specimen have been used for c_p calculation. All experiments were repeated thrice, and average values were calculated.

Thermal conductivity and diffusivity were measured using the specimens with a diameter of 8 cm and thickness of 1 cm by a multipurpose apparatus (ISOMET, Applied Precision, Bratislava, Slovakia). The measurements were made at 20 °C using a flat probe. The data were calculated automatically from the time dependence of the thermal flow in the material. The standard deviations are 5%.

2.6. Wettability Investigation

Sample wettability was analyzed using an optical contact angle measuring system OCA35 (Dataphysics, Filderstadt, Germany). Three test liquids, water, formamide, and ethylene glycol, were used to measure contact angle, surface free energy, and polar and dispersive components using Owens, Wendt, Rabel, and Kaelble method [36]. The 3 µL of each liquid was dispensed onto the sample surface, and the contact angle at room temperature was captured after 3 s (reaching thermodynamic equilibrium). A minimum of 5 measurements were recorded, and the mean value of the contact angle was obtained. All measurements were collected using SCA202 V.4.4.1 Dataphysics software.

2.7. Adhesion Characterization

The peel resistance of the sample determined the adhesion characteristics of SSPCMs samples. The peel test is performed at an angle of 90° using LF-Plus (Lloyd Instruments, West Sussex, UK) following ASTM D6862-11(2021) (Figure 1) [37]. The sample dimension was 20 × 6 mm. One side of the prepared laminate was safely placed on the instrument mobile clamp using double-adhesive tape. The Al foil was attached to the upper clamp. The test was conducted by peeling the top Al foil from the HDPE/Wax/EG at a crosshead speed of 10 mm/min. The test duration was 6 min while the top layer was delaminated entirely from the sample surface. Three independent runs were performed to obtain an average value of peel resistance and standard deviation.
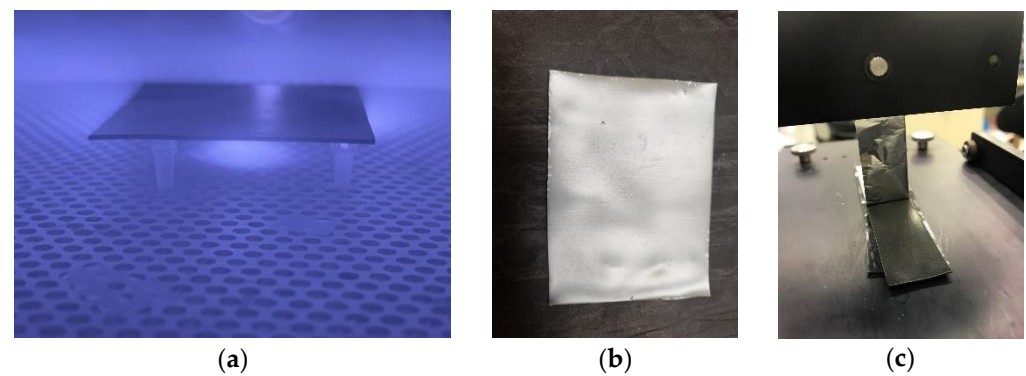
(**a**)   (**b**)   (**c**)

Figure 1. HDPE/Wax/EG Al laminate preparation and adhesion analysis: (**a**) Plasma treatment of HDPE/Wax/EG; (**b**) Prepared laminate; (**c**) Peel test.

2.8. Leakage Test

The leakage test was conducted to investigate the time dependence of the wax weight loss from the SSPCMs at the temperature over the melting point of wax according to the following procedure [35]. The strips of SSPCMs specimens with dimensions of 60 mm × 60 mm × 1 mm were placed in an oven at 60 °C for 10 days. The samples were weighed daily using an analytical balance after cleaning them from excessive and melted wax on the top surfaces with a cloth. The weight loss percentage of the wax component in the SSPCMs specimens was calculated according to Equation (1) [38]:

$$Weight\ loss\ of\ wax = ((m_0 - m)/(m_0 w)) \times 100\ (\%) \tag{1}$$

where m_0 is the initial specimen mass, m is the specimen's actual mass, and w is the mass fraction of wax.

3. Results and Discussion

3.1. Thermophysical Properties

The mechanical and thermomechanical properties of similar SSPCMs can be found in our previous papers [35,39,40]. Table 1 summarizes the selected thermophysical properties of HDPE and SSPCMs. SSPCMs have been fabricated by fixed content of wax to 50 wt.%, which is an ideal balance in terms of having adequate capacity to store and release thermal energy while maintaining good mechanical compactness of SSPCMs. EG content varied to study its influence on thermal properties and the leakage stability of SSPCMs. Thermal properties of various grades of PE mainly depend on the degree of crystallinity and temperature. HDPE used in this study has a thermal conductivity (λ) of 0.46 W/m.K, thermal diffusivity (k) of 0.330 m²/s, and a c_p of 1.81 J/g.K. The dependences of thermal capacity in both solid and molten states except phase transition region can be described by linear dependences [41].

Table 1. Selected properties of SSPCMs at 22 °C.

HDPE/WAX/EG (wt.%/wt.%/wt.%)	λ (W/m.K)	k (m²/s)	Density (kg/m)	c_p (J/kg.K)	ΔH_m (kJ/kg)	ΔH_c (kJ/kg)	T_m (°C)
100/0/0	0.46	0.3295	950	1.81 (±0.01)	NA	NA	NA
50/50/0	0.38	0.2384	925	2.27 (±0.10)	49.8 (±2.4)	48.2 (±1.8)	43.2 (0.1)
48/50/2	0.45	0.2689	951	2.23 (±0.15)	45.0 (±0.4)	44.0 (±0.3)	43.4 (0.2)
45/50/5	0.61	0.3484	990	2.16 (±0.08)	46.1 (±2.9)	45.4 (±2.1)	42.9 (0.4)
43/50/7	0.64	0.3542	1054	2.05 (±0.07)	42.5 (±1.0)	41.4 (±1.6)	43.2 (0.2)
40/50/10 *	0.81	0.4351	1055	1.98 (±0.06)	42.7 (±1.0)	40.6 (±0.6)	43.0 (0.2)

* All the parameters measured for the 40/50/10 mixture modified by 2 wt.% of OREVAC (the material, which was subsequently used for lamination) are the same within an experimental error as the unmodified 40/50/10 mixture.

The λ of graphite is not a single, unique number as it depends on the source of graphite, its purity, and structure and displays a significant anisotropy. In case the distribution of graphite flakes within a polymeric matrix is homogeneous, an effective value of thermal conductivity can be used to average thermal conductivities in various directions. For EG, the literature refers to the range of λ from 25 to 470 W/m.K [42].

The λ, as well as the thermal diffusivity of semicrystalline polymers (wax can be considered as a low molecular polyolefin in this case), depends on the degree of crystallinity. Polymers having a low/middle degree of crystallinity (up to ca. 30%–40% of crystalline phase have a λ in the range from 0.1 to 0.25 W/m.K showing very little temperature dependence. More crystalline polymers (50%–80%) have λ ranging from 0.25 to 0.9 W/m.K, and their temperature dependence is more pronounced. In this case, λ decreases with an increase in temperature, and after melting it reaches λ, which is typical for all amorphous materials, e.g., around 0.1 W/m.K [41,43]. The λ of HDPE was estimated at 0.46 W/m.K, which is in line with work published elsewhere [31]. Adding 50 wt.% of wax to HDPE caused a drop of λ to 0.38 W/m.K due to the lower λ of wax (0.2 W/m.K). The addition of EG caused an increase in λ as EG is a highly thermally conductive filler. Adding 2 wt.% of EG caused a slight increase of λ to 0.46 W/m.K. As the EG concentration increased λ also increased, reaching 0.81 W/m.K for SSPCMs containing 10 wt.%. The k followed a similar trend as λ, where k for HDPE was 0.3295 m^2/s. Adding 50 wt.% of wax caused a decrease of k to 0.2384 m^2/s, followed by increasing of k with increasing of EG content, and k for 10 wt.% of EG reached 0.4351 m^2/s.

The dependence of specific density, or more commonly tested, the specific volume of polyolefin-like polymers on temperature, is more pronounced than λ, showing a sharp first-order transition at melting temperature as a consequence of a discontinuity in volume. The specific density of common PEs is in the range from 0.9 to 0.98 g/cm^3, depending on the degree of crystallinity. The specific densities of the amorphous and fully crystalline phases of PE were determined as 0.854 g/cm^3 and 0.997 g/cm^3, respectively. The specific density of PE can be estimated using Eierman's additive rule [44], knowing the degree of crystallinity of the semicrystalline material. The increase in temperature over T_m leads to the decrease in the specific density to the values of 0.72–0.75 g/cm^3. [41,45].

The density of SSPCMs blends was determined by the addition rule based on densities of neat elements such as HDPE (0.950 kg/cm^3), wax (0.9 g/cm^3), and EG (2.25 g/cm^3). The c_p of both PE and wax, as well as their mixtures, is the most dependent on temperature due to a large first-order phase transition near a melting point due to a discontinuity in entropy. The c_p dependence on temperature is shown in Figure 2. As for the specific enthalpy of melting (ΔH_m) and the specific enthalpy of crystallization (ΔH_c), these parameters characterize a phase transition and depend on the degree of crystallinity [41].

DSC has measured c_p as well. Neat HDPE has c_p 1.81 J/kg.K, which corresponds with the literature [39]. Adding wax caused a slight increase of c_p since c_p of wax is 2.8 J/kg.K at a temperature of 22 °C. Adding EG caused decreasing in c_p from 2.23 J/kg.K for a blend having 2 wt.% EG to 1.98 J/kg.K for a blend with 10 wt.% of EG due to low c_p of neat EG. An active element of SSPCMs is wax, which can store or release thermal energy while changing from solid to liquid phase and vice versa. Phase change temperature is around 42 °C for melting of wax and around 38 °C for crystallization. The last two columns of Table 1 summarize melting and crystalizing enthalpies, ΔH_m, and ΔH_c of wax. The ΔH_m of 100% crystalline PE was found to be 288 J/g [46].

Neat HDPE does not have any phase transition at 42 °C. However, SSCPMs, having relatively high wax content, exhibited a melting peak close to 42 °C. SSPCMs containing 50 wt.% of wax have ΔH_m 39.4 kJ/kg and ΔH_c 40.0 kJ/kg. Adding EG caused a slight decrease in ΔH_m and ΔH_c. This phenomenon could be due to penetrating wax within EG graphene layers, which can influence wax's ability to crystallize [40].
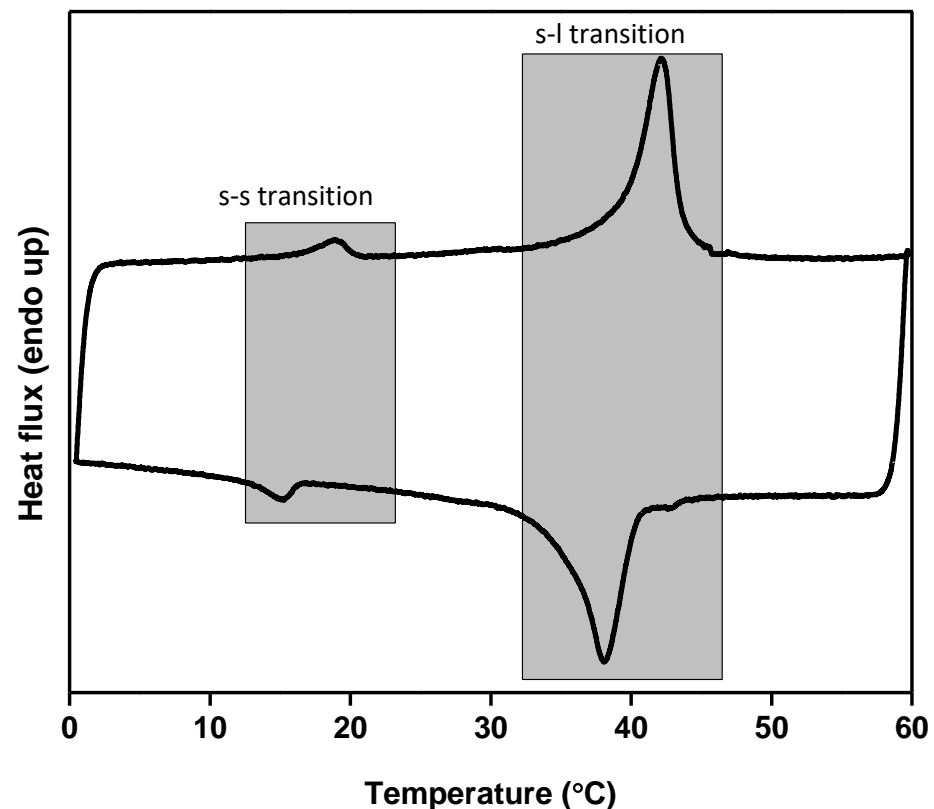
Figure 2. DSC scan of HDPE/Wax/EG (40/50/10).

DSC characterizes heat absorption and release during heating and cooling. Heat evolution of the blend and cooling of the blend is shown in Figure 2, where one minor and one main peak are observed in the heating and cooling cycle. A minor peak around 18 °C (cooling 13 °C) is attributed to the solid-solid transition of wax. The main peak of wax is at 42 °C (cooling 37 °C) and belongs to the solid-liquid transition of wax. This topic was investigated and described in our previous papers [35,47], and it was found that charging and discharging is a reversible processes, as confirmed by DSC during 150 cycles.

3.2. Leakage Test

Wax leaks from SSPCMs if the polymer blend undergoes several melting/crystallization cycles. The main reason for the leakage of paraffin wax from polymers is the inherent immiscibility of polymer/wax components and the very low molecular weight of wax in comparison to PE. This leads to the diffusion of wax from the bulk SSPCMs to its interface. The best polymer for SSPCMs preparation is PE due to its chemical and structural similarity. However, most PE grades are immiscible with wax in the crystalline phase. PE/Wax is miscible in a molten state; however, they undergo phase separation during solidification due to different morphologies of crystallites. The leakage of PCMs from the compact shape of SSPCMs is a major issue that limits their industrial applications and needs to be addressed. The wax leakage from SSPCMs was analyzed periodically every day for up to 10 days at a temperature of 60 °C, which is 18 °C higher temperature than the melting point of the wax. The results are summarized in Figure 3, showing the weight loss of SSPCMs that contain 50 wt.% of wax and various EG contents over time. Wax leakage from blends without EG is much more pronounced than from those filled with EG. It was also found that the leakage decreased with an increase in EG content. The most significant weight loss occurred during the first 2 days of the leakage experiment, where wax is released close to the surface. The most stable SSPCMs with leakage after 10 days, 7.7 wt.%, was observed for blends containing 10 wt.% of EG. This phenomenon, decreasing paraffin wax's leakage with increasing EG content, has been observed and examined in more detail in

our previous studies. The wax leakage was inversely proportional to the EG content in the linear low-density PE SSPCMs. The effect of 40 wt.% wax content in SSPCMs with several EG combinations (0 wt.%, 5 wt.%, and 10 wt.%) was studied. The presence of EG stabilized the SSPCMs directly and prevented leakage [29,35,40]. Even though 10 wt.% of EG significantly decreased wax leakage from the SSPCMs blend, other strategies must be employed to make SSPCMs suitable for industrial applications. The lamination of the finally shaped product by Al foil was explored in this study. The lamination is a straightforward method of reducing leakage, but it suffers from poor adhesion between polymer-based blends and protecting layers. Two strategies, plasma treatment or bulk modification with OREVAC additive primer, have enhanced mutual adhesiveness between HDPE/Wax/EG and Al foil. The surface treatment or bulk modification was investigated on the selected material composition of 40/50/10 (HDPE/Wax/EG). As seen in Figure 3, both approaches for improving mutual SSPCMs/Al adhesion exhibited significant leakage suppression. The test was done for up to three days, and the final leakage was 0.5 wt.% for SSPCMs laminate prepared using plasma treatment and only 0.2 wt.% for SSPCMs laminate prepared by using OREVAC additive.
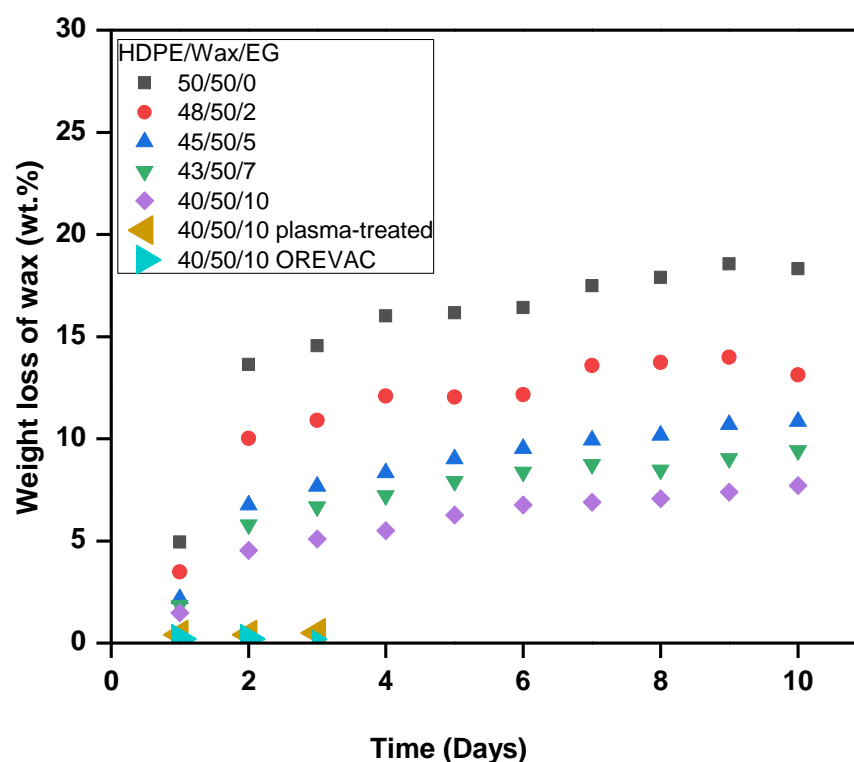

Figure 3. The leakage experiment of SSPCMs.

3.3. Surface Morphology

The information about the morphology and miscibility of the particular components in the cross-section of SSPCMs was obtained by scanning electron microscope (SEM). The SEM cross-sectional images of the SSPCMs blend containing 50 wt.% of HDPE and 50 wt.% of wax and SSPCMs blend with 40 wt.% of HDPE, 50 wt.% of wax, and 10 wt.% of EG are shown in Figure 4. SSPCMs containing only HDPE and wax (Figure 4a) clearly showed two separated phases indicating mutual immiscibility of HDPE and wax, which is one of the requirements for SSPCMs because the melting point of the polymeric matrix has to be significantly higher than the melting point of wax in order to maintain the solid, compact shape of SSPCMs after wax melting. The immiscibility of both components is demonstrated by two distinguished phase transition peaks, as confirmed by DSC analysis. Figure 4b represents SSPCMs with 5 wt.% of EG, clearly showing EG particles surrounded by HDPE

and wax. Moreover, as was already published, wax can penetrate inside EG to get between the graphene layer of EG [40].
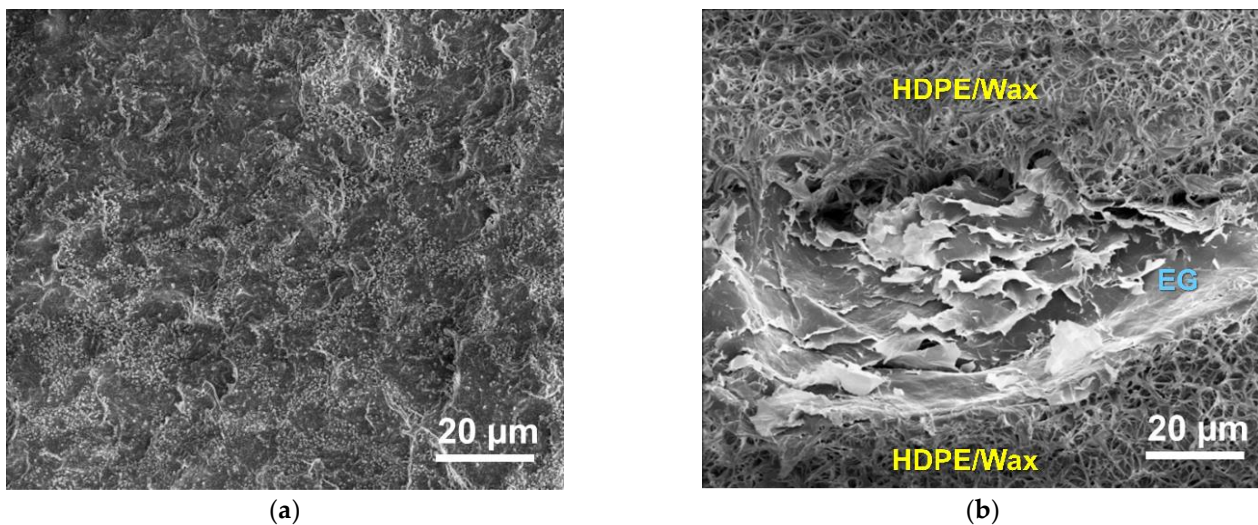

Figure 4. SEM images of SSPCMs: (**a**) 50/50 (HDPE/Wax); (**b**) 40/50/10 (HDPE/Wax/EG).

3.4. Chemical Composition

The Fourier transform infrared (FTIR) technique was used to analyze the chemical composition of unmodified and modified HDPE samples, and representative FTIR spectra are shown in Figure 5. An FTIR spectrum of neat HDPE contains characteristic absorbance bands associated with hydrocarbon chains and branches, such as vibrations in-CH_2-/-CH stretching and bending at approximately 2915–2845 cm^{-1}, 1470–1460 cm^{-1} asymmetric and 730–719 cm^{-1} rocking. Plasma treatment of HDPE led to the appearance of a new absorbance band at a maximum of 1714 cm^{-1} associated with C=O due to the surface functionalization processes. The intensity of the C=O absorbance band was even more evident in the HDPE/Wax/EG RF sample. Moreover, the FTIR spectrum showed absorbance bands of-OH and O-C=O after plasma treatment. Adding wax and EG to HDPE resulted in a new absorbance band with a maximum of 890 cm^{-1} wavenumber. Adding OREVAC to HDPE/Wax/EG showed only a slight presence of polar functional groups in the FTIR spectrum, probably caused by bulk modification, while the top layer mainly consisted of HDPE, wax, or EG were mainly present.

3.5. Adhesion

The peel resistance between Al and HDPE, HDPE/Wax, HDPE/Wax/EG before and after plasma treatment, and HDPE/Wax/EG OREVAC are shown in Figure 6. The hydrophobic and inert surface of HDPE led to poor adhesion to Al, while peel resistance was 0.5 N/m. Plasma treatment of HDPE and Al resulted in a significant increase in peel resistance (54.1 N/m). Incorporating wax and EG into HDPE led to a slight increase in peel resistance (2.2 N/m) of HDPE/Wax/EG sample compared with unmodified HDPE, mainly due to an effect of solid wax present on the surface of HDPE adhered to Al foil. Additional plasma treatment of HDPE/Wax/EG increased adhesive characteristic to Al foil slightly; peel resistance was 7.2 N/m. The best adhesive characteristic was achieved for HDPE/Wax/EG samples modified by adhesive promoter OREVAC, while peel resistance increased to 55.1 N/m.
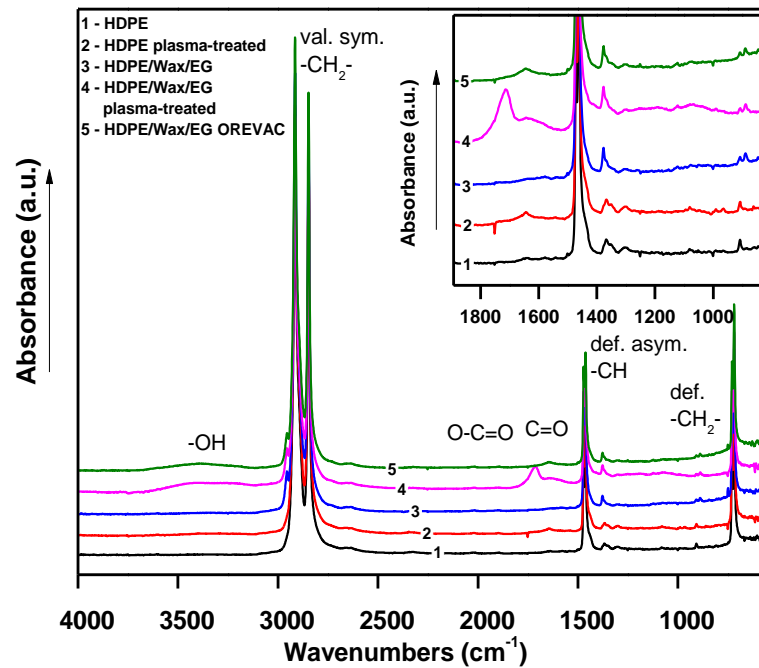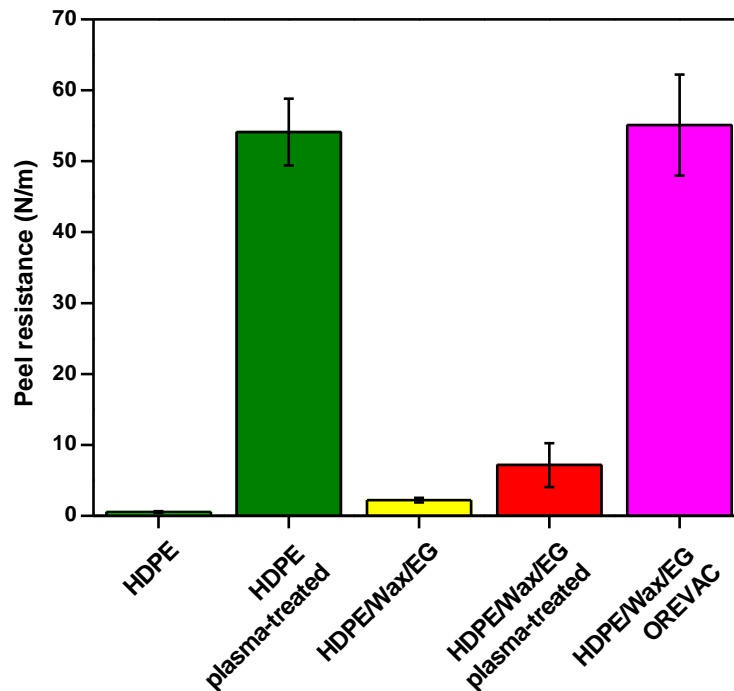
Figure 5. FTIR spectra of SSPCMs samples.

Figure 6. Peel test of SSPCMs samples with Al.

3.6. Wettability

The surface properties of SSPCMs samples concerning the plasma treatment or modification by maleated PE were determined by contact angle measurements, and the results are summarized in Figure 7. Three testing liquids with different surface tension (water, formamide, and ethylene glycol) were used to evaluate surface free energy providing information about wettability. The water contact angle for the unmodified HDPE sample was above 90°, indicating hydrophobic behavior, the same as high contact angles for formamide (82.4°) and ethylene glycol (68.2°) liquids as well. Therefore, according to them, evaluated surface free energy and its polar and dispersive components achieved low values equal to

25.8 mJ/m^2, 2.4 mJ/m^2, and 23.4 mJ/m^2, respectively. The contact angles of the plasma-treated HDPE sample were significantly decreased due to etching and functionalization processes, while the contact angle of water, formamide, and ethylene glycol achieved 45.6°, 27.2°, and 31.8°, respectively, which is considered a hydrophilic character. As a result, the surface free energy and its polar component increased to 54.0 and 48.8 mJ/m^2, respectively, while the dispersive component decreased to 8.1 mJ/m^2. A similar trend was observed in the case of the HDPE/Wax/EG and HDPE/Wax/EG plasma-treated samples. However, the wettability of HDPE decreased after adding wax and EG, while the contact angle of water, formamide, and ethylene increased to 112.0°, 93.6°, and 89.1°, respectively, because of the additives' effect on the surface and morphology properties [48]. As a result, the surface free energy and polar component decreased to 18.8 mJ/m^2 and 0.4 mJ/m^2. Conversely, HDPE/Wax/EG plasma-treated excelled by contact angles of 42.6°, 42.4°, and 43.4° for water, formamide, and ethylene glycol, respectively, while the surface free energy and polar component was 62.9 mJ/m^2 and 61.46 mJ/m^2. Modifying the HDPE/Wax/EG sample with OREVAC did not result in significant changes, as maleated PE was present in bulk, while the top layer consisted mainly of HDPE/Wax or EG, which was confirmed by FTIR measurements. The above results prove that plasma treatment improves the hydrophilic properties of the HDPE samples after 1 min of plasma treatment time. Plasma treatment is essential in concurrently improving the adhesion and surface contact between polymer and metal materials.
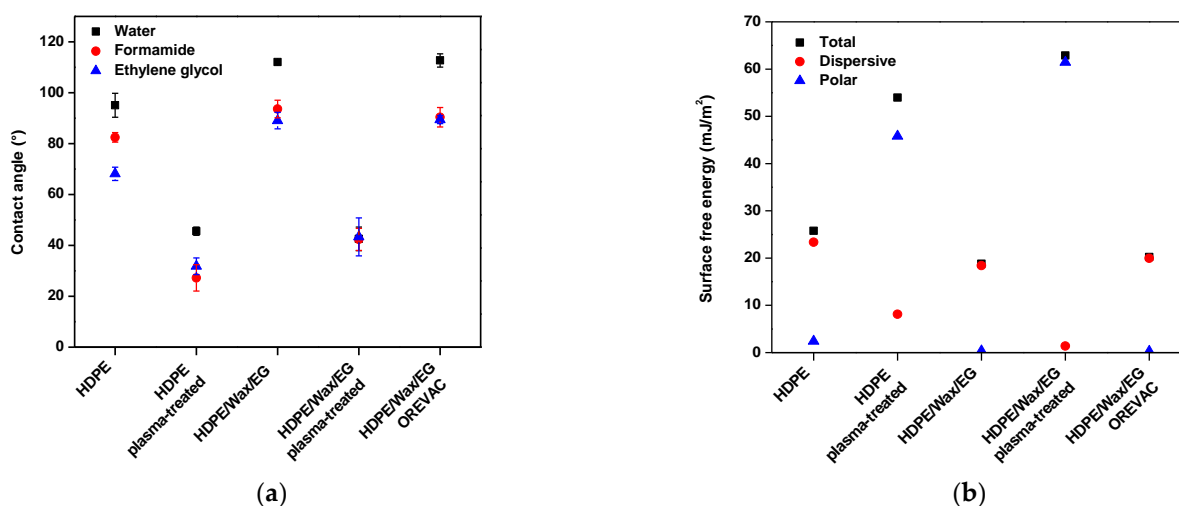

Figure 7. Wettability analyses of SSPCMs: (**a**) Contact angle; (**b**) Surface free energy.

4. Conclusions

The unique solution for paraffin wax leakage from polymeric SSPCMs formed by HDPE and wax blends by lamination with Al foil was reported in this study, aiming for an enhancement of compositional stability SSPCMs. The lamination of SSPCMs by Al foil was investigated as the simplest method of reducing leakage, but it suffers from poor adhesion between polymer-based blends and protecting layers. In this study, the improved adhesion between SSPCMs and plasma-treated Al foil was achieved by plasma treatment of SSPCMs or adding maleated PE acting as an adhesion promoter into SSPCMs:

- The peel resistance of SSPCMs after plasma treatment or modification by maleated PE, which characterizes the strength of the adhesion joint, was 7.2 N/m or 55.1 N/m, respectively. As a result, wax leakage from the laminated SSPCMs was suppressed significantly.
- The plasma-treated or maleated PE-modified SSPCMs showed leakage of 0.5 wt.% or 0.2 wt.%, respectively, after three days of leakage test, representing a significant enhancement of the leakage suppression caused by Al lamination.

Both plasma treatment and the incorporation of a small amount of maleated polymer are realizable at a large, industrial scale. Moreover, adding 2 wt.% of the adhesion promoter

does not influence the thermal properties of SSPCMs. These findings indicate a good potential for industrially applied SSPCMs.

Nomenclature

Abbreviation		Symbols	
SSPCMs	Shape-stabilized phase change materials	c_p	Specific heat capacity (J/kg.K)
PCMs	Phase change materials	ΔH_m	Melting enthalpy (kJ/kg)
HDPE	High-density polyethylene	ΔH_c	Crystalline Enthalpy (kJ/kg)
EG	Expanded graphite	T_m	Melting temperature (°C)
Al	Aluminum	m_0	Initial specimen mass
TES	Thermal energy storage	m	Actual specimen mass
PE	Polyethylene	w	Mass fraction of wax
UV	Ultraviolet	λ	Thermal conductivity (W/m.K)
OREVAC	Maleated polyethylene	k	Thermal diffusivity (m^2/s)
RF	Radio-frequency		
DSC	Differential scanning calorimetry		
FTIR	Fourier transform infrared		
SEM	Scanning electron microscope		
RT	Room temperature		

References

1. UNEP SBCI Buildings and Climate Change Status, Challenges and Opportunities. Available online: https://wedocs.unep.org/handle/20.500.11822/7783;jsessionid=08AAA5916A7FAC01CB3BF2AC417BD313 (accessed on 23 October 2022).
2. Gunasekara, S.N.; Barreneche, C.; Inés Fernández, A.; Calderón, A.; Ravotti, R.; Ristić, A.; Weinberger, P.; Ömur Paksoy, H.; Koçak, B.; Rathgeber, C.; et al. Thermal energy storage materials (Tesms)—What does it take to make them fly? *Crystals* **2021**, *11*, 1276. [CrossRef]
3. Liu, G.; Xiao, T.; Guo, J.; Wei, P.; Yang, X.; Hooman, K. Melting and solidification of phase change materials in metal foam filled thermal energy storage tank: Evaluation on gradient in pore structure. *Appl. Therm. Eng.* **2022**, *212*, 118564. [CrossRef]
4. Liu, G.; Li, Y.; Wei, P.; Xiao, T.; Meng, X.; Yang, X. Thermo-Economic Assessments on a Heat Storage Tank Filled with Graded Metal Foam. *Energies* **2022**, *15*, 7213. [CrossRef]
5. Frigione, M.; Sarcinella, A.; Luis, J.; De Aguiar, B. Development and Performance of Eco-Sustainable Form-Stable Phase Change Materials (PCMs) for Mortars to Be Applied in Buildings Located in Different Climatic Areas. *Coatings* **2023**, *13*, 258. [CrossRef]
6. Tyagi, V.V.; Chopra, K.; Sharma, R.K.; Pandey, A.K.; Tyagi, S.K.; Ahmad, M.S.; Sarı, A.; Kothari, R. A comprehensive review on phase change materials for heat storage applications: Development, characterization, thermal and chemical stability. *Sol. Energy Mater. Sol. Cells* **2022**, *234*, 111392. [CrossRef]

7. Hassan, F.; Jamil, F.; Hussain, A.; Ali, H.M.; Janjua, M.M.; Khushnood, S.; Farhan, M.; Altaf, K.; Said, Z.; Li, C. Recent advancements in latent heat phase change materials and their applications for thermal energy storage and buildings: A state of the art review. *Sustain. Energy Technol. Assess.* **2022**, *49*, 101646. [CrossRef]

8. Kenisarin, M.; Mahkamov, K. Solar energy storage using phase change materials. *Renew. Sustain. Energy Rev.* **2007**, *11*, 1913–1965. [CrossRef]

9. Zalba, B.; Marín, J.M.; Cabeza, L.F.; Mehling, H. Review on thermal energy storage with phase change: Materials, heat transfer analysis and applications. *Appl. Therm. Eng.* **2003**, *23*, 251–283. [CrossRef]

10. Khudhair, A.M.; Farid, M.M. A review on energy conservation in building applications with thermal storage by latent heat using phase change materials. *Energy Convers. Manag.* **2004**, *45*, 263–275. [CrossRef]

11. Hasnain, S.M. Review on sustainable thermal energy storage technologies, part I: Heat storage materials and techniques. *Energy Convers. Manag.* **1998**, *39*, 1127–1138. [CrossRef]

12. Zhang, X.X.; Fan, Y.F.; Tao, X.M.; Yick, K.L. Fabrication and properties of microcapsules and nanocapsules containing n-octadecane. *Mater. Chem. Phys.* **2004**, *88*, 300–307. [CrossRef]

13. Ben Hamad, G.; Younsi, Z.; Naji, H.; Salaün, F. A comprehensive review of microencapsulated phase change materials synthesis for low-temperature energy storage applications. *Appl. Sci.* **2021**, *11*, 11900. [CrossRef]

14. Fan, Y.F.; Zhang, X.X.; Wu, S.Z.; Wang, X.C. Thermal stability and permeability of microencapsulated n-octadecane and cyclohexane. *Thermochim. Acta* **2005**, *429*, 25–29. [CrossRef]

15. Lin, X.; Zhang, X.; Ji, J.; Liu, L.; Yang, M.; Zou, L. Experimental investigation of form-stable phase change material with enhanced thermal conductivity and thermal-induced flexibility for thermal management. *Appl. Therm. Eng.* **2022**, *201*, 117762. [CrossRef]

16. Meng, L.; Ivanov, A.S.; Kim, S.; Zhao, X.; Kumar, N.; Young-Gonzales, A.; Saito, T.; Bras, W.; Gluesenkamp, K.; Bocharova, V. Alginate-Sodium Sulfate Decahydrate Phase Change Composite with Extended Stability. *ACS Appl. Polym. Mater.* **2022**, *4*, 6563–6571. [CrossRef]

17. Peng, G.; Dou, G.; Hu, Y.; Sun, Y.; Chen, Z. Phase change material (PCM) microcapsules for thermal energy storage. *Adv. Polym. Technol.* **2020**, *2020*, 9490873. [CrossRef]

18. Takai-Yamashita, C.; Shinkai, I.; Fuji, M.; EL Salmawy, M.S. Effect of water soluble polymers on formation of Na_2SO_4 contained SiO_2 microcapsules by W/O emulsion for latent heat storage. *Adv. Powder Technol.* **2016**, *27*, 2032–2038. [CrossRef]

19. Pasupathi, M.K.; Alagar, K.; Michael Joseph Stalin, P.; Matheswaran, M.M.; Aritra, G. Characterization of Hybrid-nano/Paraffin Organic Phase Change Material for Thermal Energy Storage Applications in Solar Thermal Systems. *Energies* **2020**, *13*, 5079. [CrossRef]

20. Manoj Kumar, P.; Mylsamy, K.; Saravanakumar, P.T. Experimental investigations on thermal properties of nano-SiO_2/paraffin phase change material (PCM) for solar thermal energy storage applications. *Energy Sources, Part A Recover. Util. Environ. Eff.* **2020**, *42*, 2420–2433. [CrossRef]

21. Kaushik, N.; Saravanakumar, P.; Dhanasekhar, S.; Saminathan, R.; Rinawa, M.L.; Subbiah, R.; Sharma, R.; Manoj Kumar, P. Thermal analysis of a double-glazing window using a Nano-Disbanded Phase Changing Material (NDPCM). *Mater. Today Proc.* **2022**, *62*, 1702–1707. [CrossRef]

22. Krupa, I.; Nógellová, Z.; Špitalský, Z.; Janigová, I.; Boh, B.; Sumiga, B.; Kleinová, A.; Karkri, M.; Almaadeed, M.A. Phase change materials based on high-density polyethylene filled with microencapsulated paraffin wax. *Energy Convers. Manag.* **2014**, *87*, 400–409. [CrossRef]

23. Sari, A. Form-stable paraffin/high density polyethylene composites as solid-liquid phase change material for thermal energy storage: Preparation and thermal properties. *Energy Convers. Manag.* **2004**, *45*, 2033–2042. [CrossRef]

24. Cheng, F.; Xu, Y.; Lv, Z.; Huang, Z.; Fang, M.; Liu, Y.; Wu, X.; Min, X. Form-stable and tough paraffin-Al_2O_3/high density polyethylene composites as environment-friendly thermal energy storage materials: Preparation, characterization and analysis. *J. Therm. Anal. Calorim.* **2021**, *146*, 2089–2099. [CrossRef]

25. Krupa, I.; Miková, G.; Luyt, A.S. Polypropylene as a potential matrix for the creation of shape stabilized phase change materials. *Eur. Polym. J.* **2007**, *43*, 895–907. [CrossRef]

26. Krupa, I.; Luyt, A.S. Physical properties of blends of LLDPE and an oxidized paraffin wax. *Polymer* **2001**, *42*, 7285–7289. [CrossRef]

27. Krupa, I.; Luyt, A.S. Thermal properties of uncross-linked and cross-linked LLDPE/wax blends. *Polym. Degrad. Stab.* **2000**, *70*, 111–117. [CrossRef]

28. Kalnæs, S.E.; Jelle, B.P. Phase change materials and products for building applications: A state-of-the-art review and future research opportunities. *Energy Build.* **2015**, *94*, 150–176. [CrossRef]

29. Sobolčiak, P.; Abdelrazeq, H.; Ouederni, M.; Karkri, M.; Al-Maadeed, M.A.; Krupa, I. The stabilizing effect of expanded graphite on the artificial aging of shape stabilized phase change materials. *Polym. Test.* **2015**, *46*, 65–71. [CrossRef]

30. AlMaadeed, M.A.; Labidi, S.; Krupa, I.; Karkri, M. Effect of expanded graphite on the phase change materials of high density polyethylene/wax blends. *Thermochim. Acta* **2015**, *600*, 35–44. [CrossRef]

31. Guo, Y.; Ruan, K.; Shi, X.; Yang, X.; Gu, J. Factors affecting thermal conductivities of the polymers and polymer composites: A review. *Compos. Sci. Technol.* **2020**, *193*, 108134. [CrossRef]

32. (PDF) DuPont r PCM Guidebook_December 2010—PDFSLIDE.NET. Available online: https://pdfslide.net/documents/dupont-r-pcm-guidebookdecember-2010.html (accessed on 6 January 2023).

33. Sobolciak, P.; Karkri, M.; Al-Maadeed, M.A.; Krupa, I. Thermal characterization of phase change materials based on linear low-density polyethylene, paraffin wax and expanded graphite. *Renew. Energy* **2016**, *88*, 372–382. [CrossRef]
34. Kunisada, R. Density measures and additive property. *J. Number Theory* **2017**, *176*, 184–203. [CrossRef]
35. Krupa, I.; Nógellová, Z.; Špitalský, Z.; Malíková, M.; Sobolčiak, P.; Abdelrazeq, H.W.; Ouederni, M.; Karkri, M.; Janigová, I.; Al-Maadeed, M.A.S.A. Positive influence of expanded graphite on the physical behavior of phase change materials based on linear low-density polyethylene and paraffin wax. *Thermochim. Acta* **2015**, *614*, 218–225. [CrossRef]
36. Owens, D.K.; Wendt, R.C. Estimation of the surface free energy of polymers. *J. Appl. Polym. Sci.* **1969**, *13*, 1741–1747. [CrossRef]
37. Conshohocken, W. Standard Test Method for 90 Degree Peel Resistance of Adhesives 1. Available online: https://www.astm.org/d6862-11r21.html (accessed on 1 January 2023).
38. Krupa, I.; Sobolčiak, P.; Abdelrazeq, H.; Ouederni, M.; Al-Maadeed, M.A. Natural aging of shape stabilized phase change materials based on paraffin wax. *Polym. Test.* **2017**, *63*, 567–572. [CrossRef]
39. Sobolčiak, P.; Abdulgader, A.; Mrlik, M.; Popelka, A.; Abdala, A.A.; Aboukhlewa, A.A.; Karkri, M.; Kiepfer, H.; Bart, H.J.; Krupa, I. Thermally conductive polyethylene/expanded graphite composites as heat transfer surface: Mechanical, thermo-physical and surface behavior. *Polymers* **2020**, *12*, 2863. [CrossRef]
40. Sobolciak, P.; Mrlík, M.; Almaadeed, M.A.; Krupa, I. Calorimetric and dynamic mechanical behavior of phase change materials based on paraffin wax supported by expanded graphite. *Thermochim. Acta* **2015**, *617*, 111–119. [CrossRef]
41. Van Krevelen, D.W. *Properties of Polymers: Their Correlation with Chemical Structure; Their Numerical Estimation and Prediction from Additive Group Contributions*, 4th ed.; Elsevier: Amsterdam, The Netherlands, 2009; ISBN 9780080548197.
42. Murugan, P.; Nagarajan, R.D.; Shetty, B.H.; Govindasamy, M.; Sundramoorthy, A.K. Recent trends in the applications of thermally expanded graphite for energy storage and sensors—A review. *Nanoscale Adv.* **2021**, *3*, 6294–6309. [CrossRef]
43. Eiermann, K. Bestimmung der Temperaturabhängigkeit des Kristallisationsgrades aus der Wärmeleitfähigkeit. *Kolloid-Z. Z. Polym.* **1964**, *198*, 96–98. [CrossRef]
44. Eiermann, K. Modellmäßige Deutung der Wärmeleitfähigkeit von Hochpolymeren—Teil 3: Teilkristalline Hochpolymere. *Kolloid-Z. Z. Polym.* **1965**, *201*, 3–15. [CrossRef]
45. Compass. Available online: https://compass.astm.org/document/?contentCode=ASTM%7CD3418-21%7Cen-US&proxycl=https%3A%2F%2Fsecure.astm.org&fromLogin=true (accessed on 6 January 2023).
46. Wunderlich, B. *Macromolecular Physics Vol. 1: Crystal Structure, Morphology, Defects*; Academic Press: New York, NY, USA, 1973; Volume 1, ISBN 9780127656014.
47. Lachheb, M.; Mustapha, K.; Fethi, A.; Sassi, B.N.; Magali, F.; Patrik, S. Thermal properties measurement and heat storage analysis of paraffin/graphite composite phase change material. *Compos. Part B Eng.* **2014**, *66*, 518–525. [CrossRef]
48. Popelka, A.; Khanam, P.N.; Almaadeed, M.A. Surface modification of polyethylene/graphene composite using corona discharge. *J. Phys. D Appl. Phys.* **2018**, *51*, 105302. [CrossRef]